ACS APPLIED MATERIALS & INTERFACES

RESEARCH ARTICLE

www.acsami.org

CuO Codoped ZnO Based Nanostructured Materials for Sensitive Chemical Sensor Applications

Mohammed M. Rahman,* Aslam Jamal, Sher Bahadar Khan, and Mohd Faisal

Center for Advanced Materials and Nano-Engineering (CAMNE) and Department of Chemistry, Faculty of Sciences and Arts, Najran University, P.O. Box 1988, Najran 11001, KSA

ABSTRACT: Due to numerous potential applications of semiconductor transition metal−doped nanomaterials and the great advantages of hydrothermal synthesis in both cost and environmental impact, a significant effort has been employed for growth of copper oxide codoped zinc oxide (CuO codoped ZnO) nanostructures via a hydrothermal route at room conditions. The structural and optical properties of the CuO codoped ZnO nanorods were characterized using various techniques such as UV−visible, Fourier transform infrared (FT-IR) spectroscopy, X-ray diffraction (XRD), field emission scanning electron microscopy (FE-SEM), etc. The sensing performance has been executed by a simple and reliable $I-V$ technique, where aqueous ammonia is considered as a target analyte. CuO codoped ZnO nanorods of thin film with conducting coating agents on silver electrodes (AgE, surface area of 0.0216 cm^2) displayed good sensitivity, stability, and reproducibility. The calibration plot is linear over the large dynamic range, where the sensitivity is approximately $1.549 \pm 0.10\ \mu A\ cm^{-2}\ mM^{-1}$ with a detection limit of $8.9 \pm 0.2\ \mu M$, based on signal/noise ratio in short response time. Hence, on the bottom of the perceptive communication between structures, morphologies, and properties, it is displayed that the morphologies and the optical characteristics can be extended to a large scale in transition-metal-doped ZnO nanomaterials and efficient chemical sensors applications.

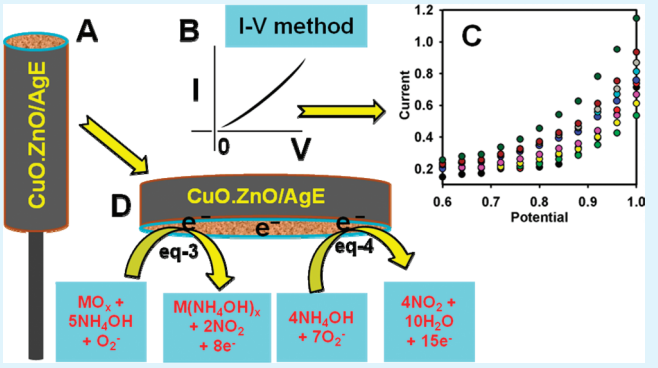

KEYWORDS: CuO codoped ZnO nanorods, hydrothermal method, powder X-ray diffraction, aqueous ammonia sensors, sensitivity, $I-V$ technique

INTRODUCTION

Nanomaterials have attracted a wide interest owing to their unique properties and immense potential application in chemical sensor fabrication.[1−3] Semiconductor material has been recognized as a promising host nanomaterial for transition material at room temperature. It is revealed a stable morphological structure and composed of a number of irregular phases with geometrically coordinated metals and oxide atoms, piled alternately along the axes.[4] Transition metals codoped in semiconductor nanomaterials have concerned profound research effort for its exceptional and outstanding properties and versatile applications.[5−7] Recently, an extensive development has been made on the research leading of metal-oxide codoped ZnO-based nanomaterials actuated by both fundamental sciences and prospective advanced technologies.[8] The doped semiconductor nanostructures exhibit promising uses as field consequence transistors,[9] UV photodetectors,[10] gas sensors,[11] field emission electron sources,[12] nanomaterials,[13] nanoscale power generators,[14] and many other functional devices.[15] The transition metal doped nanostructure is also a competent method to regulate the energy level surface states of ZnO, which can further progress by the changes in doping concentrations of doped semiconductor materials.

Chemical sensing quest has been investigated with the metal oxide nanostructures for the detection of different chemicals such as hydrazine, methanol, chloroform, dichloromethane, acetone, ethanol, etc., which are not environmentally friendly. The sensing mechanism with doped or undoped metal oxide thin films utilized mainly the properties of porous film formed by the physi-sorption and chemisorption techniques. The chemical detection is based on the current changes of the fabricated thin films caused by the chemical components of the reacting system in aqueous medium.[16−20] The main efforts are focused on detecting the minimum quantity aqueous ammonia necessary for the fabricated doped sensors for electrochemical investigation. Nanomaterials offer many opportunities of tuning the chemical sensing properties.

In the present study, it is employed that the hydrothermal method prepares copper oxide codoped zinc oxide nanomaterials with nearly controlled rod-shape structure, which revealed a continuous morphological advancement in nanostructure materials and potential applications. With most of the contemporary works focused on undoped ZnO, there has been more and more attention dedicated to explore the doped counterparts. For semiconductor nanomaterials, doping is an influential appliance to conform the optical and electrical properties, expediting the development of many electronic and optoelectronic devices.

Received: February 3, 2011
Accepted: March 28, 2011
Published: March 28, 2011

Semiconductor nanostructure CuO codoped ZnO nanorods allow very sensitive transduction of the liquid/surface interactions into a change in the electrochemical properties. The possibility to form a variety of structural morphologies suggests different prospects of tuning the chemical sensing properties. CuO codoped ZnO nanomaterial is fabricated into a simple and efficient chemical sensor consisting of a side-polished silver electrode surface and measuring the chemical sensing performance in aqueous ammonia at room conditions. To best of our knowledge, this is the first report for detection of aqueous ammonia with calcined CuO codoped ZnO nanomaterials using a simple and reliable $I-V$ method in a short response time.

EXPERIMENTAL SECTION

Materials and Methods. Copper chloride, zinc chloride, ammonia solution (25%), butyl carbitol acetate, ethyl acetate, monosodium phosphate, disodium phosphate, and all other chemicals used were of analytical grade and obtained from Sigma-Aldrich Company. The λ_{max} (301.0 nm) of calcined CuO codoped ZnO nanorod materials was assessed with UV−visible spectroscopy (Lamda-950, Perkin-Elmer, Germany). Fourier transform infrared (FT-IR) spectra were confirmed with a spectrophotometer (Spectrum-100 FT-IR) in the mid-IR range, which was purchased from Perkin-Elmer, Germany. The powder X-ray diffraction (XRD) patterns were measured with an X-ray diffractometer (XRD; X'Pert Explorer, PANalytical diffractometer) equipped with Cu Kα1 radiation (λ = 1.5406 nm) using a generator voltage of 40 kV, and a generator current of 35 mA was applied for the determination. Morphology of CuO codoped ZnO was recorded on a field emission scanning electron microscopy instrument (FE-SEM; JSM-7600F, Japan). The $I-V$ technique is investigated using an electrometer (Kethley, 6517A, Electrometer, USA).

Synthesis of CuO Codoped ZnO Nanorods. CuO codoped ZnO nanomaterials have been synthesized by adding unimolar concentration of copper chloride and zinc chloride precursor into a hydrothermal cell (Teflon line autoclave) for 16 h. Copper chloride and zinc chloride were slowly dissolved into the deionized water separately to make 0.1 M concentration at room temperature. Then, these equi-molar solutions were mixed gently and stirred until mixed properly. The solution pH was slowly adjusted dropwise in an alkaline system. Then, the mixture was put into a hydrothermal cell to put in the oven for a longer time and maintained the temperature. The starting materials of $ZnCl_2$, $CuCl_2$, and NH_4OH were used without further purification for the coprecipitation method to CuO codoped into ZnO. The NH_4OH was added dropwise into the vigorously stirred $ZnCl_2$ and $CuCl_2$ solution mixture to produce a white precipitate.

The growth mechanism of the nanomaterials could be apprehended on the basis of chemical reactions and nucleation, as well as development of ZnO crystals. The apparent reaction mechanisms are proposed for obtaining the doped nanomaterial oxides, which are presented below.

$$NH_4OH_{(aq)} \rightarrow {NH_4}^{+}{}_{(aq)} + {OH}^{-}{}_{(aq)} \quad \text{(i)}$$

$$ZnCl_{2(s)} + 2{OH}^{-}{}_{(aq)} \rightarrow Zn(OH)_{2(aq)} + 2{Cl}^{-}{}_{(aq)} \quad \text{(ii)}$$

$$Zn(OH)_{2(aq)} + 2NH_4OH_{(aq)} \rightarrow {ZnO_2}^{-1}{}_{(aq)} + 2{NH_4}^{+}{}_{(aq)} + 2H_2O \quad \text{(iii)}$$

$$CuCl_{2(aq)} + 4NH_4OH_{(aq)} + {ZnO_2}^{-1}{}_{(aq)} \rightarrow CuO\cdot ZnO_{(s)} + 4{NH_4}^{+}{}_{(aq)} + 2{Cl}^{-}{}_{(aq)} + 2H_2O \quad \text{(iv)}$$

$$Zn(OH)_{2(aq)} + CuO_{(aq)} \rightarrow CuO\cdot ZnO(s) + H_2O \quad \text{(v)}$$

The precursors of $CuCl_2$ and $ZnCl_2$ are soluble in alkaline medium (NH_4OH reagent) according to the equations of i−iii. After addition of NH_4OH into the mixture of metal oxides solution, it was stirred gently for a few minutes at room temperature. Then, the solution pH is adjusted (10.3) using NH_4OH and put into an autoclave cell to set into the oven at 150.0 °C for 16 h, where the active temperature of the solution mixture is approximately in the range of 90.0−100.0 °C. The reaction is progressed slowly according to the eqs iv and v. Then, the solution was washed thoroughly with acetone and kept drying at room temperature.

During the total synthesis process, NH_4OH acts a pH buffer to regulate the pH value of the solution and slow supply of OH^- ions.[21] When the concentration of the Zn^{2+} and OH^- ions are reached over the critical value, the precipitation of ZnO nuclei initiates. As there is high concentration of Cu^{2+} ion in the solution, the nucleation of ZnO crystals forms by coprecipitation, owing to the lower activation energy barrier of heterogeneous nucleation. However, as the concentration of Cu^{2+} was present in the mixture of solution, some larger ZnO crystals with a rod-like morphology developed among the nanostructures, which was composed of CuO codoped ZnO nanomaterials. The shape of CuO codoped calcined ZnO rods is approximately consistent with the growth habit of ZnO crystals.[22,23] Finally, the as-grown CuO codoped ZnO nanomaterials were calcined at 400.0 °C for 5 h in the furnace (Barnstead Thermolyne, 6000 Furnace, USA). The calcined products were characterized in detail in terms of their morphological, structural, and optical properties and applied for ammonia chemical sensing.

Fabrication and Detection Technique of Aqueous Ammonia. Phosphate buffer solution (PBS; 0.1 M) at pH 7.0 is prepared by mixing 0.2 M Na_2HPO_4 and 0.2 M NaH_2PO_4 solution in 100.0 mL of deionized water. A silver electrode is fabricated with calcined nanomaterials, where butyl carbitol acetate (BCA) and ethyl acetate (EA) are the conducting coating agents. Then, it is transferred into the oven at 70.0 °C for 6 h until the film is completely uniform and dried. An electrochemical cell is mounted with nanomaterial coated AgE as a working electrode and Pd wire as a counter electrode. Ammonia solution (25%) is diluted at different concentrations in DI water and used as a target. The amount of 0.1 M PBS was kept constant in the beaker as 10.0 mL throughout the chemical investigation. Analyte solution is prepared with various concentrations of aqueous ammonia from 77.0 μM to 7.7 M. The sensitivity is calculated from the slope of current vs concentration (I vs C) from the calibration plot divided by the value of active surface area of sensors/electrodes. An electrometer is used as a voltage source for the $I-V$ technique in a two electrode system.

RESULTS AND DISCUSSION

UV−Visible and FT-IR Spectroscopy. The optical absorption spectra of CuO codoped ZnO samples are executed using a UV−vis spectrophotometer in the visible range. The absorption spectrum of calcined nanomaterial solution is presented in Figure 1A. It represents the absorption maxima at 301.0 nm in the visible range between 200.0 and 800.0 nm wavelengths, which indicated the formation of CuO codoped ZnO nanorod formation by the hydrothermal route.[24] Band gap energy is calculated on the basis of the maximum absorption band of CuO codoped ZnO nanomaterials and obtained to be 4.1196 eV, according to following equation.

$$E_{bg} = \frac{1240}{\lambda}\ (\text{eV})$$

where E_{bg} is the band gap energy and λ_{max} is the wavelength (301.0 nm) of the nanomaterials.

The calcined CuO codoped ZnO nanomaterials is also characterized from the atomic and molecular vibrations.

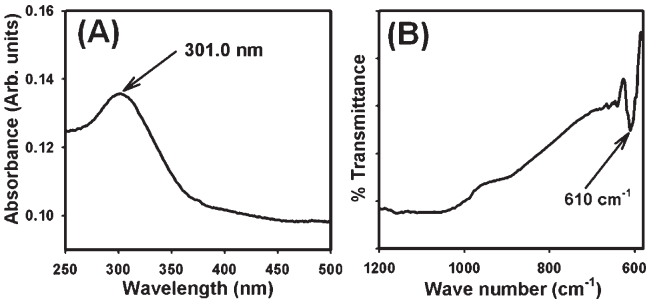

Figure 1. (A) UV−visible spectroscopy and (B) FT-IR spectroscopy of calcined CuO codoped ZnO nanomaterials.

To anticipate the actuated recognitions clearly, FT-IR spectra only in the region of 400−4000 cm^{-1} are employed. Figure 1B represents the FT-IR spectrum of the calcined nanomaterials. It exhibits a band at 610 cm^{-1}. This observed vibration band may be assigned as metal−oxygen−metal (M−O−M) stretching vibration. The observed vibration bands at low frequency regions suggest the formation of metal−oxide nanomaterials.

FE-SEM and Powder X-ray Diffraction. High resolution FE-SEM images of calcined CuO codoped ZnO nanomaterials are presented in Figure 2A−C. The images are composed of nanostructure materials with nanorod shapes. The rod and aggregated-rod shapes exhibited the zinc-oxide and copper-oxide nanostructures, respectively. In Figure 2A, the diameter of ZnO nanorods is calculated in the range of 280.0−800.0 nm, where the average value is close to 530.0 ± 20.0 nm. In Figure 2B, the size of the aggregated nanorods grown by copper oxide materials is close to 8.0 μm. The diameter of inner rods of aggregated copper materials is 183.0 ± 10.0 nm. It is clear from the FE-SEM images that the hydrothermally synthesized products are nanostructures of CuO codoped ZnO, which propagated in a very high density and possessed nanorod shapes. Figure 2C represents the high-resolution (magnified) FE-SEM image of the calcined nanomaterials. It is reflected that most of the nanostructures are possessed in rod shapes of the aggregated copper nanomaterials.

The CuO codoped ZnO nanopowder samples were analyzed and exhibited as wurtzite structure with hexagonal shapes. The sample was calcined at 400.0 °C in a furnace to ascertain the formation of nanocrystalline phases. Figure 2C shows typical crystallinity of the calcined CuO codoped ZnO nanorods and their aggregation. All the reflection peaks in this pattern were found to match with ZnO phase (zincite) having hexagonal geometry [JCPDF # 071-6424]. The phases showed the major characteristic peaks (black color) with indices for calcined crystalline ZnO at 2θ values of 31.8(100), 34.5(002), 36.4(101), 47.8(102), 56.7(110), 63.0(103), 66.2(200), 69.1(201), and 89.6(203) degrees. The hexagonal (unit cell) lattice parameters are a = 3.2494, b = 5.2038, point group of $P63mc$, and radiation of Cu Kα1 (λ = 1.5406). These indicate that there is a significant amount of crystalline ZnO present in nanomaterials. The reflection peaks were observed to match with CuO phase (Tenorite) being base-centered monoclinic [JCPDF # 073-6234]. The phases represented the major characteristic peaks (blue color) with indices for calcined crystalline CuO at 2θ values of 32.7(110), 35.8(−111), 38.9(111), 46.4(−112), 48.0(−202), 53.8(020), 58.4(202), 61.8(−113), and 68.1(113), 73.5(221), 75.4(−222), 80.4(−114), and 83.7(312) degrees. The monoclinic lattice parameters are a = 4.662, b = 3.417, c = 5.118, β = 99.48, point group of $C2/c$, and radiation of Cu Kα1 (λ = 1.5406). These indicate that there is a significant amount of crystalline CuO present in nanomaterials. The diffraction patterns of calcined samples can be indexed to the hexagonal structure of ZnO. The other peaks corresponding to CuO related secondary phase were found in a copper oxide doped sample, which may be attributed to the incorporation of CuO into the ZnO lattice site.

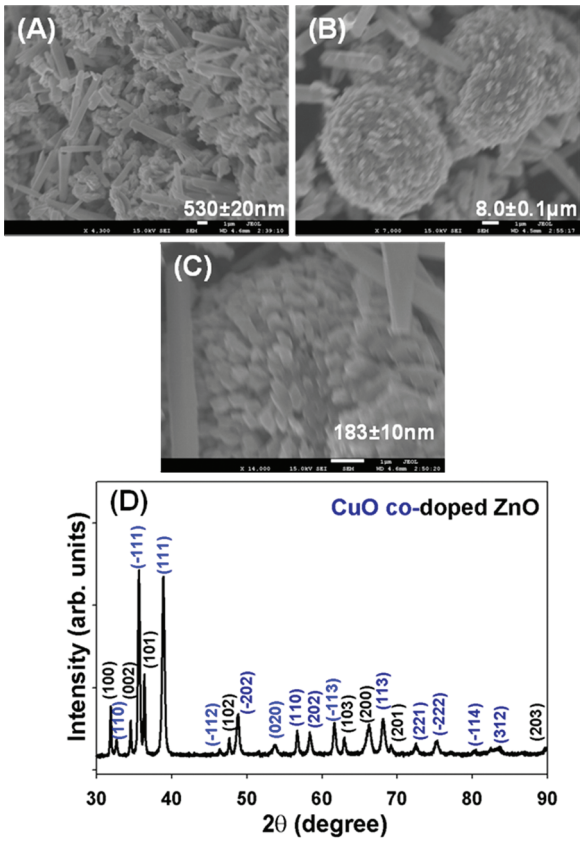

Figure 2. (A−C) Low to high magnified FE-SEM images and (D) powder X-ray diffraction pattern of calcined CuO codoped ZnO.

Detection of Aqueous Ammonium Using *I*−*V* Technique. The potential application of CuO codoped ZnO nanostructures as chemical sensors has been explored for detecting and quantifying hazardous chemicals, which are not environmentally friendly. Development of doping of this nanostructure materials as chemi-sensors is in the primitive stage, and only a limited number of reports are available.[25−27] The nanorods of CuO codoped ZnO chemi-sensors have advantages such as stability in air, nontoxicity, chemical stability, electrochemical activity, ease to fabricate, and biosafe characteristics. As in the case of chemical sensors, the principle of operation is that the current response in I−V technique of CuO codoped ZnO nanorod drastically changes when aqueous ammonia is adsorbed.

The calcined CuO codoped ZnO nanomaterials were used for fabrication of chemical sensor, where aqueous ammonia was considered as target analyte. The emaciated film of nanomaterial sensor was fabricated with conducting agents and embedded on the silver electrode surface, which is presented in Figure 3A. The fabricated electrode was accumulated in the oven at low temperature (70.0 °C) for a few hours to dry, stable, and uniform the film totally. The electrical responses of target analyte were executed using the I−V method, which is presented in

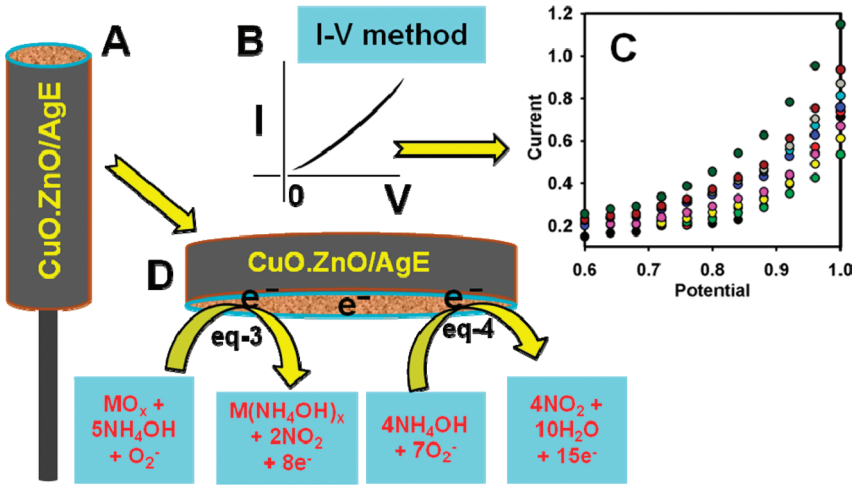

Figure 3. Schematic view of (A) fabrication of AgE with coating agents, (B) detection of $I-V$ method (theoretical), (C) outcomes of $I-V$ experimental result, (D) proposed mechanisms of aqueous ammonia detection in the presence of semiconductor CuO codoped ZnO nanomaterials.

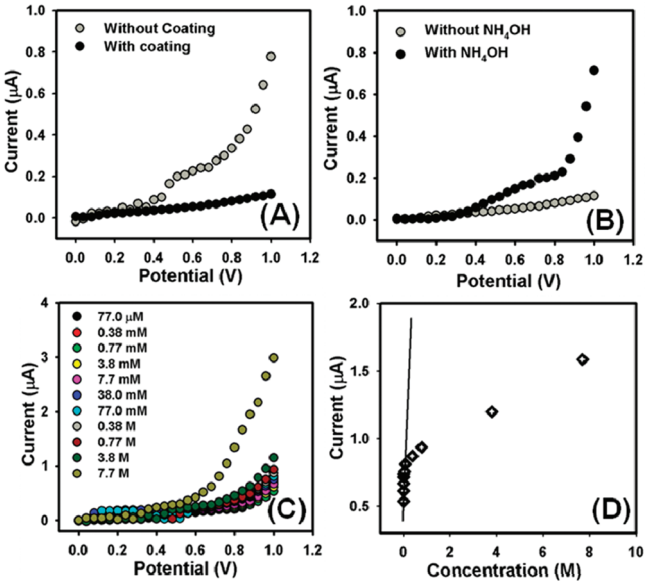

Figure 4. $I-V$ responses of (A) without and with coating; (B) in absence and presence of aqueous ammonia; (C) concentration variations (77.0 μM to 7.7 M) of analyte; and (D) calibration plot of CuO codoped ZnO nanomaterials fabricated on AgE surfaces. Potential was taken between 0 and +1.0 V.

Figure 3B. Hypothetical and experimental $I-V$ responses[28,29] of a chemical sensor having CuO codoped ZnO thin film as a function of current versus potential for aqueous ammonia, which is shown in Figure 3B,C, respectively. The time delaying of electrometer was kept for 1.0 s. A significant increase in the current value with applied potential is clearly demonstrated.

Figure 4A shows the current changing without (gray dotted) and with (dark dotted) coating of CuO codoped ZnO on silver electrodes. With the nanomaterial coating electrode, the $I-V$ response is reduced compared to that without the coating electrode, which means the surface is slightly inhibited with metal oxides. The gray-dotted (without) and dark-dotted (with) curves indicate the responses of the modified film before and after injecting of 50.0 μL of aqueous ammonia in 10.0 mL of PBS

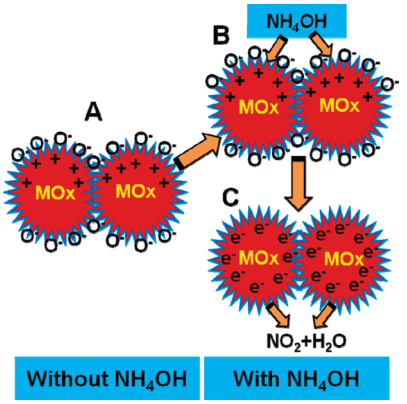

Figure 5. Mechanism of CuO codoped ZnO chemical sensors at ambient conditions.

solution, respectively, which is presented in Figure 4B. The significant change of surface current is measured in each injection of the target component into the bulk solution. PBS solution (10.0 mL; 0.1 M) is initially taken into the cell, and the low to high concentrations of aqueous ammonia are added dropwise sequentially from the stock solution. $I-V$ responses on fabricated CuO codoped ZnO surface are measured from the various concentrations of aqueous ammonia (77.0 μM to 7.7 M), which is presented in the Figure 4C. It shows the current responses of coated films as a function of ammonium hydroxide concentration at room temperature. It is observed that, at low to high concentration of target analyte, the current increases gradually. A wide range of analyte concentration is selected to study the possible analytical parameters, which is calculated in 77.0 μM to 7.7 M. The calibration curve was plotted from the variation of analyte concentrations, which is presented in the Figure 4D. The sensitivity is calculated from the calibration curve, which is close to 1.549 $\pm$ 0.10 μA cm^{-2} mM^{-1}. The linear dynamic range of this sensor exhibits from 77.0 μM to 0.77 M, and the detection limit was around 8.9 $\pm$ 0.2 μM [3 $\times$ noise(N)/slope(S)].

The aqueous ammonia sensing mechanism of CuO codoped ZnO sensors is based on the semiconductors oxides, due to oxidation or reduction of the semiconductor oxide itself,

according to the dissolved O_2 in bulk solution or surface air of the surrounding atmosphere.

$$e^- (\text{semiconductor materials}) + O_2 \rightarrow O_2^- \quad (1)$$

$$e^- (\text{semiconductor materials}) + O_2^- \rightarrow 2O^- \quad (2)$$

These reactions take place in bulk solution or air/liquid interface or surrounding air due to the low carrier concentration which increased the resistance. The NH_4OH sensitivity toward CuO codoped ZnO (e.g., MO_x) could be attributed to the high oxygen deficiency, and defect density led to increased oxygen adsorption. The larger the amount of oxygen adsorbed on the surface, the larger would be the oxidizing capability and faster would be the oxidation of NH_4OH. The reactivity of NH_4OH would have been very large as compared to another chemical with the surface under the same condition.[30] When NH_4OH reacts with the adsorbed O_2 on the doped surface of the film, it gets oxidized to nitrogen oxide gas and metal ammonium hydroxide, liberating free electrons in the conduction band which could be expressed through the following reactions:

$$MO_x + 5NH_4OH + O_2^- \rightarrow M(NH_4OH)_x + 2NO_{2(g)} + 8e^- (\text{C.B.}) \quad (3)$$

$$4NH_4OH + 7O_2^- \rightarrow 4NO_2 + 10H_2O + 15e^- \quad (4)$$

These reactions corresponded to oxidation of the reducing carriers. These processes increased the carrier concentration and consequently reduced the resistance on exposure to reducing liquids/analytes. At the room condition, the exposure of metal oxide surface to reducing liquid/analytes results in a surface mediated combustion process. The elimination of iono-sorbed oxygen enhances the electron density as well as the surface conductance of the film.[31] The reducing analyte (NH_4OH) donates electrons to the CuO codoped ZnO surface. Therefore, resistance decreases, or conductance increases. This is why the analyte response (current response) increases with increasing potential. It shows an n-type conduction mechanism, which is proposed in the Figure 5. Thus, produced electrons supply to rapidly enhance conductance of the thick film. The CuO codoped ZnO eccentric regions dispersed on the surface would enhance the ability of material to absorb more oxygen species giving high resistance in ambient air.

The response time was around 10 s for the CuO codoped ZnO coated-electrode to reach saturated steady state current. The high sensitivity of film can be attributed to the good absorption (porous surfaces fabricated with coating), adsorption ability, high catalytic activity, and good biocompatibility of the CuO codoped ZnO nanomaterials. The estimated sensitivity of the fabricated sensor is relatively higher than previously reported ammonium hydroxide sensors based on other composite or material modified electrodes.[32−34] Due to large surface area, the nanomaterials provided a favorable nanoenvironment for the chemical detection with good quantity. The high sensitivity of CuO codoped ZnO provided high electron communication features which improved the direct electron transfer between the active sites of nanomaterials and AgE. The modified thin film had a good stability. Additionally, due to high specific surface area, the nanorods of CuO codoped ZnO impart a favorable environment for the aqueous ammonia detection (by adsorption) with large quantity. The high sensitivity of nanomaterials provides high electron communication aspects which promote the direct electron communication between the active sites of nano CuO codoped ZnO and AgE.

CuO codoped ZnO reveals some prospective in providing chemical based sensors, and encouraging progress has been executed in the research segment. Despite this progress, there are still a number of important issues that require further investigation before this material can be transferred to commercial use for the stated applications. As for the nanomaterials, CuO codoped ZnO nanorods provide a path to a new generation of chemical sensors, but a premeditated effort has to be expended for doped nanostructures to be taken critically for large scale applications and to achieve high appliance density with accessibility to individual sensors. Reliable methods for fabricating, assembling, and integrating building blocks onto sensors need to be explored.

CONCLUSIONS

This chloride-based hydrothermal method resembles a universal attitude to fabricate transition-metal-doped ZnO nanomaterials with preeminent morphologies. Such a controlled doping has extensive presumption and perturbs the crystalline and electronic structures of zinc oxide. It is also a successfully fabricated highly sensitive ammonia sensor based on calcined CuO codoped ZnO embedded AgE with conducting binders, for the first time. CuO codoped ZnO nanorods are selectively prepared hydrothermally with reducing agents in alkaline medium, which represents a simple, easy, convenient, and economical approach. An aqueous ammonia sensor is studied by a simple $I-V$ technique at room condition, and the analytical performances are investigated thoroughly in terms of sensitivity, detection limit, response time, and storage stability. The crystalline structure, shapes, optical properties, and band gap were investigated by XRD, FE-SEM, and UV−visible techniques. This contribution provided extensive research activities that convened on the synthesis, characterization, and chemical sensing application of CuO codoped ZnO nanorods. This new approach also introduced a new route for efficient chemical sensor development to control the environmental toxicity carcinogenicity and could also play an important role in biomedical health care fields.

AUTHOR INFORMATION

Corresponding Author

*E-mail: mmrahman@nu.edu.sa and mmrahmanh@gmail.com.

ACKNOWLEDGMENT

We greatly acknowledge Najran University for their financial support and research facilities. Centre for Advanced Materials and Nano-Engineering (CAMNE), Najran University, Najran, is greatly acknowledged for their chemicals and nanomaterial analyses.

REFERENCES

(1) Wang, X.; Song, J.; Liu, J.; Wang, Z. L. *Science* **2007**, *316*, 102.
(2) Keren, K.; Berman, R. S.; Buchstab, E.; Sivan, U.; Braun, E. *Science* **2003**, *302*, 1380.
(3) Umar, A.; Rahman, M. M.; Al-Hajry, A.; Hahn., Y. B. *Talanta* **2009**, *78*, 284.
(4) Chakraborti, D.; Narayan, J.; Prater, J. T. *Appl. Phys. Lett.* **2007**, *90*, 062504.

(5) Umar, A.; Rahman, M. M.; Kim, S. H; Hahn., Y. B. *Chem. Commun.* **2008**, 166.
(6) Rahman, M. M.; Jamal, A.; Khan, S. B.; Faisal, M. *J. Nanopart. Res.* **2011**, DOI:10.1007/s11051-011-0301-7.
(7) Hara, K.; Horiguchi, T.; Kinoshita, T.; Sayama, K.; Sugihara, H.; Arakawa, H. *Sol. Energy Mater. Sol. Cells* **2000**, *64*, 115.
(8) Wang, Z. L. *J. Phys.: Condens. Matter* **2004**, *16*, R829.
(9) Ng, H. T.; Han, J.; Yamada, T.; Nguyen, P.; Chen, Y. P.; Meyyappan, M. *Nano Lett.* **2004**, *4*, 1247.
(10) Soci, C.; Zhang, A.; Xiang, B.; Dayeh, S. A.; Aplin, D. P. R.; Park, J.; Bao, X. Y.; Lo, Y. H.; Wang, D. *Nano Lett.* **2007**, *7*, 1003.
(11) Li, Q. H.; Liang, Y. X.; Wan, Q.; Wang, T. H. *Appl. Phys. Lett.* **2004**, *85*, 6389.
(12) Lee, C. J.; Lee, T. J.; Lyu, S. C.; Zhang, Y.; Ruh, H.; Lee, H. J. *Appl. Phys. Lett.* **2002**, *81*, 3648.
(13) Huang, M. H.; Mao, S.; Feick, H.; Yan, H.; Wu, Y.; Kind, H.; Weber, E.; Russo, R.; Yang, P. *Science* **2001**, *292*, 1897.
(14) Wang, X. D.; Song, J. H.; Liu, J.; Wang, Z. L. *Science* **2007**, *316*, 102.
(15) Zhang, Z.; Yi, J. B.; Ding, J.; Wong, L. M.; Seng, H. L.; Wang, S. J.; Tao, J. G.; Li, G. P.; Xing, G. Z.; Sum, T. C.; Huan, C. H. A.; Wu., T. *J. Phys. Chem. C* **2008**, *112*, 9579.
(16) Ansari, S. G.; Wahab, R.; Ansari, Z. A.; Kim, Y. S.; Khang, G.; Al-Hajry, A.; Shin., H. S. *Sens. Actuators, B* **2009**, *137*, 566.
(17) Lee, S. R.; Rahman, M. M.; Ishida, M.; Sawada., K. *Trends Anal. Chem.* **2009**, *28*, 196.
(18) Rahman, M. M.; Umar, A.; Sawada., K. *Sens. Actuators, B* **2009**, *137*, 327.
(19) Lee, S. R.; Rahman, M. M.; Ishida, M.; Sawada., K. *Biosen. Bioelectron.* **2009**, *24*, 1877.
(20) Rahman, M. M.; Hasnat, M. A.; Sawada, K. *J. Sci. Res.* **2009**, *1*, 108.
(21) Strom, J. G. J.; Jun, H. W.; Pharm, J. *J. Pharm. Sci.* **1980**, *69*, 1261.
(22) Wang, R. C.; Lin., H. Y. *Mater. Chem. Phys.* **2011**, *125*, 263.
(23) Laudise, R. A.; Ballman, A. A. *J. Phys. Chem.* **1960**, *64*, 688.
(24) Pankove, J. I. *Optical process in Semiconductors*; Prentice-Hall: Upper Saddle River, NJ, 1971.
(25) Dulub, O.; Meyer, B.; Diebold, U. *Phys. Rev. Lett.* **2005**, *95*, 136101.
(26) Al-Hillia, S. M.; Willander, M.; Öst, A.; Strålfors, P. *J. Appl. Phys.* **2007**, *102*, 084304.
(27) Al-Hilli, S. M.; Al-Mofarji, R. T.; Willander, M. *Appl. Phys. Lett.* **2006**, *89*, 173119-1.
(28) Ansari, S. G.; Ansari, Z. A.; Wahab, R.; Kim, Y. S.; Khang, G.; Shin., H. S. *Biosens. Bioelectron.* **2008**, *23*, 1838.
(29) Faisal, M.; Khan, S. B.; Rahman, M. M.; Jamal. A. *Mater. Lett.* **2011**, *65*, 1400.
(30) Patil, D. R.; Patil, L. A.; Amalnerkar., P. P. *Bull. Mater. Sci.* **2007**, *30*, 553.
(31) Mujumdar, S. *Mater. Sci. Poland* **2009**, *27*, 123.
(32) Dikovska, A. O.; Atanasova, G. B.; Nedyalkov, N. N.; Stefanov, P. K.; Atanasov, P. A.; Karakoleva, E. I.; Andreev, A. T. *Sens. Actuators, B* **2010**, *146*, 331.
(33) Raj, V. B.; Nimal, A. T.; Parmar, Y.; Sharma, M. U.; Sreenivas, K.; Gupta, V. *Sens. Actuators, B* **2010**, *147*, 517.
(34) Raj, K.; Moskowitz, B.; Casciari, R. *J. Magn. Magn. Mater.* **1995**, *149*, 174.

NOTE ADDED AFTER ASAP PUBLICATION

This paper was published on the Web on April 6, 2011, with missing information in refs 32 and 33 in the original version. The corrected version was reposted on April 11, 2011.